Biol Cybern (2013) 107:217–232
DOI 10.1007/s00422-013-0547-5

ORIGINAL PAPER

Biological Cybernetics

Measuring frequency domain granger causality for multiple blocks of interacting time series

Luca Faes · Giandomenico Nollo

Received: 29 November 2011 / Accepted: 11 January 2013 / Published online: 29 January 2013

Abstract In the past years, several frequency-domain causality measures based on vector autoregressive time series modeling have been suggested to assess directional connectivity in neural systems. The most followed approaches are based on representing the considered set of multiple time series as a realization of two or three vector-valued processes, yielding the so-called Geweke linear feedback measures, or as a realization of multiple scalar-valued processes, yielding popular measures like the directed coherence (DC) and the partial DC (PDC). In the present study, these two approaches are unified and generalized by proposing novel frequency-domain causality measures which extend the existing measures to the analysis of multiple blocks of time series. Specifically, the block DC (bDC) and block PDC (bPDC) extend DC and PDC to vector-valued processes, while their logarithmic counterparts, denoted as multivariate total feedback f^{m} and direct feedback g^{m}, represent into a full multivariate framework the Geweke's measures. Theoretical analysis of the proposed measures shows that they: (i) possess desirable properties of causality measures; (ii) are able to reflect either direct causality (bPDC, g^{m}) or total (direct + indirect) causality (bDC, f^{m}) between time series blocks; (iii) reduce to the DC and PDC measures for scalar-valued processes, and to the Geweke's measures for pairs of processes; (iv) are able to capture internal dependencies between the scalar constituents of the analyzed vector processes. Numerical analysis showed that the proposed measures can be efficiently estimated from short time series, allow to represent in an objective, compact way the information derived from the causal analysis of several pairs of time series, and may detect frequency domain causality more accurately than existing measures. The proposed measures find their natural application in the evaluation of directional interactions in neurophysiological settings where several brain activity signals are simultaneously recorded from multiple regions of interest.

Keywords Block-based connectivity analysis · Directed coherence · Granger causality · Vector autoregressive (VAR) models · Neurophysiological time series · Partial directed coherence

1 Introduction

In recent years, neuroscientists have recognized that a detailed investigation of how brain areas functionally interact is fundamental for describing the neurophysiological processes typically engaged in cognitive and perceptive processing, as well as for assessing several neurological disorders. Such an investigation, commonly referred to as the study of brain connectivity (Sporns 2007), is being favored by the fast advancement of multielectrode data acquisition technologies such as electroencephalography (EEG) and magnetoencephalography (MEG), as well as by the continuous development of multivariate time series analysis techniques (Pereda et al. 2005). In the study of brain connectivity, the issue of determining directionality of the interactions among neural signals is of great interest because it allows revealing pathways of information flow within the nervous system. In this regard, measures based on vector autoregressive (VAR) time series models have been proposed in neuroscience

L. Faes (✉)
Lab. Biosegnali, Dipartimento di Fisica & BIOtech, Università di Trento, via delle Regole 101, 38060 Mattarello, Trento, Italy
e-mail: luca.faes@unitn.it

G. Nollo
BIOtech, Dipartimento di Ingegneria Industriale, Università di Trento, and IRCS PAT-FBK, Trento, Italy

(Baccala et al. 1998; Baccala and Sameshima 2001; Chen et al. 2006; Kaminski and Blinowska 1991; Kaminski et al. 2001; Wang et al. 2007) and extensively applied to investigate multichannel neural data (Astolfi et al. 2007; Brovelli et al. 2004; Dhamala et al. 2008; Ding et al. 2007; Erla et al. 2009; Franaszczuk et al. 1994; Sato et al. 2009; Schelter et al. 2006; Winterhalder et al. 2005). These measures reflect the probabilistic notion of causality provided by Granger (1969, 1980), which covers direct causal effects from one series to another in a multivariate dataset, or related concepts taking into account not only direct but also indirect causal effects (Sims 1972). In spite of its widespread utilization in neuroscience, it is noteworthy that the concept of Granger causality is formulated in terms of predictability and, as such, is suited for empirical investigations of cause–effects relationships but does not necessarily reflect the existence of true causal effects. As there is no universally accepted definition of causality, different concepts which provide suitable frameworks for causal inference have been proposed and debated (see, e.g., Eichler 2012 for an overview relevant to time series analysis). In the context of this debate, recent works have shown that connectivity measures based on Granger causality quantify the information transfer from a statistical perspective which is quite distinct from the interventionist perspective that should be followed to infer effectively the existence of causal effects (Lizier and Prokopenko 2010; Chicharro and Ledberg 2012; Eichler 2012).

The application of Granger causality analysis to multi-electrode neural data in which several regions of interest are considered, with each region represented by a set of several recording channels, presupposes to deal with multiple and vector-valued processes underlying the acquired multiple blocks of time series. This general methodological framework has been considered by several authors, e.g., providing definitions for Granger (non)causality (Boudjellaba et al. 1992; Tjostheim 1981) and measures of feedback and conditional feedback (Geweke 1982, 1984) valid for vector processes, and proposing graphical approaches for modeling and interpreting Granger-causal relationships (Eichler 2005, 2007). Within this framework, the assessment of Granger causality between two of the multiple vector-valued processes is performed by testing for the statistical significance of the entries of the VAR coefficient submatrices corresponding to the two processes [typically using Wald tests (Lutkepohl 2005)]. While this time domain approach is straightforward and widely used, especially in econometrics (Eichler 2007; Hsiao 1982; Toda and Phillips 1993), it does not account for the fact that strength and direction of Granger-causal relations between the modeled time series may vary over different frequencies. The idea that a spectral density approach would give further insights than an overall time domain causality detection which is supposed to encompass all periodicities in the observed series was first suggested by Granger himself (1969). More recently, this idea has become the basis of many neuroscience applications motivated by the fact that Granger causality analysis performed in the frequency domain allows disclosing connectivity mechanisms operating within specific frequency bands, e.g., related to the EEG or MEG rhythms (Faes et al. 2012; Faes and Nollo 2011). On this basis, the present study is focused on the analysis of Granger causality and related concepts of total causal influence performed in the frequency domain.

Frequency domain Granger causality is expressed in terms of measures of directional connectivity defined from the spectral representation of the VAR model coefficients. In neuroscience applications, two main approaches have been followed to derive these connectivity measures. The so-called Geweke approach is based on combining the multiple available time series into two blocks considered as representative of two regions of interest, and then defining logarithmic spectral measures of Granger causality which quantify the directional relations between the two blocks (Geweke 1982; Wang et al. 2007). This approach was also extended considering a third block of time series, yielding a conditional causality measure that elicits the direct causal influence between the two blocks of interest (Chen et al. 2006; Geweke 1984). However, the Geweke measures do not pursue a truly multivariate approach to the inference of connectivity among multiple interacting blocks of time series, because they are not computed from a joint simultaneous representation of all series blocks. Therefore, their application with more channels becomes cumbersome as either many pairs or triplets of blocks have to be tested, or the conditioning block has to be constructed as a composite vector of the remaining data channels (see, e.g., Zhou et al. 2009). In a second approach, developed by the pioneering works of Kaminski et al. (Kaminski et al. 2001; Kaminski and Blinowska 1991) and Baccalà et al. (Baccala et al. 1998; Baccala and Sameshima 2001), each single time series is considered as representative of a region of interest, so that the number of series included in the VAR model corresponds to the number of underlying processes. In this way, frequency domain causality measures such as the directed coherence (DC) and the partial DC (PDC) could be defined between each pair of scalar time series within the full multivariate representation. However, the resulting measures have been set only for the study of scalar-valued processes, so that they need to be further elaborated in an arbitrary way when dealing with blocks of time series. As an example, if one wants to assess causality between two regions each characterized by more than one recording channel, DC or PDC have to be computed individually between all pairs of channels and then somehow averaged over all pairs.

The aim of the present study is to unify and generalize the above presented approaches for the frequency domain quantification of directional connectivity, by proposing new causality measures which extend the DC/PDC measures to vector-valued processes on one side, and provide a full multivariate account for the Geweke measures on the other side. The proposed measures are defined from the VAR representation of multiple vector-valued processes, and are shown to possess desirable theoretical properties of causality measures, to be able to reflect either direct or total (i.e., direct + indirect) causality from one process to another, and to reduce to the existing Geweke measures in the case of two vector-valued processes or to the DC/PDC measures in the case of multiple scalar-valued processes. The measures are illustrated in theoretical and numerical examples of multiple linearly interacting vector-valued processes. The Matlab® code for computation of the frequency domain connectivity measures defined in this paper is freely available for download at: http://www.science.unitn.it/biophysicslab/research/sigpro/block/toolbox_block.html.

2 Background

The notation for this paper is to use italic lowercase letters, italic capital letters, and bold capital letters for scalar, vector, and matrix variables, respectively. The superscripts ^{T} and * denote the transpose and conjugate transpose matrix operators, respectively. For a $Q \times Q$ matrix $\mathbf{A}$, $|\mathbf{A}|$ is the determinant, A_{ij} is the i–j scalar entry, A^*_{ij} is the complex conjugate of A_{ij} $(i, j = 1, \dots Q)$; if $\mathbf{A}$ is partitioned in M^2 blocks, $\mathbf{A}_{lm}$ is the l–m block and $\mathbf{A}^*_{lm}$ is the conjugate transpose of $\mathbf{A}_{lm}$ $(l, m = 1, \dots M)$.

Let us consider M distinct, discrete time, vector-valued stochastic processes $Y_1, \dots, Y_M$ of dimensions $M_1, \dots, M_M$, such that the mth process, Y_m, is composed of M_m zero-mean scalar-valued stationary processes: $Y_m = [y_{m1} \cdots y_{mM_m}]^T$ $(m = 1, \dots, M)$. Without loss of generality we assume that all processes are defined at discrete time ($Y_m = Y_m(n)$; e.g., are sampled versions of the continuous time processes $Y_m(t)$, taken at the times $t_n = nT$, with T the sampling period) and have zero mean ($\mathrm{E}[Y_m(n)] = 0$, where $\mathrm{E}[\cdot]$ is the statistical expectation operator). The M vector-valued processes can also be represented in a compact form through the overall vector $Y(n) = \left[Y_1(n)^T \cdots Y_M(n)^T\right]^T = \left[y_1(n) \cdots y_Q(n)\right]$ of dimension $Q = \sum_{m=1}^{M} M_m$.

Assuming that the overall process $Y(n)$ admits an autoregressive (AR) representation, it can be described by means of the linear parametric model (Lutkepohl 2005)

$$Y(n) = \sum_{k=1}^{\infty} \mathbf{A}(k) Y(n-k) + U(n), \tag{1}$$

where $\mathbf{A}(k)$ is the $Q \times Q$ matrix of the model coefficients, and $U(n) = [u_1(n) \cdots u_Q(n)]$ is a vector of Q zero-mean white and uncorrelated innovation processes with positive definite covariance matrix $\mathbf{\Sigma} = \mathrm{E}[U(n)U(n)^T]$. Every stationary process with AR representation as in (1) also has a moving average (MA) representation which lets it to be described as

$$Y(n) = \sum_{k=0}^{\infty} \mathbf{H}(k) U(n-k), \tag{2}$$

where $\mathbf{H}(k)$ is the $Q \times Q$ transfer matrix.

The spectral representation of the AR and MA process representations may be obtained taking the Fourier transform (FT) of (1) and (2), yielding $Y(\omega) = \mathbf{A}(\omega)Y(\omega) + U(\omega)$ and $Y(\omega) = \mathbf{H}(\omega)U(\omega)$, where $Y(\omega)$ and $U(\omega)$ are the FTs of $Y(n)$ and $U(n)$, and the $Q \times Q$ coefficient and transfer matrices are defined in the frequency domain as

$$\mathbf{A}(\omega) = \sum_{k=1}^{\infty} \mathbf{A}(k) \mathrm{e}^{-\mathbf{j}\omega kT}, \tag{3a}$$

$$\mathbf{H}(\omega) = \sum_{k=0}^{\infty} \mathbf{H}(k) \mathrm{e}^{-\mathbf{j}\omega kT}, \tag{3b}$$

where $\mathbf{j} = \sqrt{-1}$ for $\omega \in [-\pi, \pi)$. Comparing the two spectral representations, it is easy to show that the coefficient and transfer matrices are linked by: $\mathbf{H}(\omega) = [\mathbf{I}_Q - \mathbf{A}(\omega)]^{-1} = \bar{\mathbf{A}}(\omega)^{-1}$ ($\mathbf{I}_Q$ is the $Q \times Q$ identity matrix). According to a well-known spectral factorization theorem (Gevers and Anderson 1981), the $Q \times Q$ spectral density matrix of the overall process, $\mathbf{S}(\omega)$, as well as its inverse, $\mathbf{P}(\omega) = \mathbf{S}(\omega)^{-1}$, can be factored in terms of the transfer and coefficient matrices as

$$\mathbf{S}(\omega) = \mathbf{H}(\omega) \mathbf{\Sigma} \mathbf{H}^*(\omega), \tag{4a}$$

$$\mathbf{P}(\omega) = \bar{\mathbf{A}}^*(\omega) \mathbf{\Sigma}^{-1} \bar{\mathbf{A}}(\omega). \tag{4b}$$

As we will show in the next subsections, the factorizations in (4) provide the basis of the methods proposed so far for the frequency domain evaluation of directional interactions in jointly stationary processes. As of now we note that, to be unambiguous, the factorizations need to rely on diagonal forms for the covariance matrix $\mathbf{\Sigma}$ (and for its inverse $\mathbf{\Sigma}^{-1}$); together with whiteness of $U(n)$, the diagonality assumption corresponds to full uncorrelation, even at lag $k = 0$, of the scalar innovation processes. This condition is commonly denoted as *strict causality*, and needs to be verified in model validation, or properly handled by suitable modifications of the model structure (Faes and Nollo 2010, 2011; Geweke 1982). Dealing with the effects of instantaneous correlations is beyond the scope of the present paper; this issue deserves a thorough analysis which is being prepared for a future submission.

2.1 Causality definitions

The AR representation of vector stochastic processes expressed in (1) can be related to the notion of Granger causality

(1969, 1980), which was originally formulated stating the principles that the cause precedes the effect in time, and that the causal process contains unique information about the caused process that is not available otherwise. Following these principles, Granger causality is assessed in a VAR setting by checking that the entries of the coefficient matrices $\mathbf{A}(k)$ corresponding to the two considered processes do not vanish uniformly for all lags k (Eichler 2006; Hsiao 1982; Toda and Phillips 1993). It is noteworthy that, according to this formulation, Granger causality refers to the exclusive consideration of direct causal effects from one process to another within the multivariate representation. On the other hand, it has been recently shown (Eichler 2012) that the evaluation of both direct and indirect effects between two processes reflects the notion of causality first formulated by Sims (1972), which indeed can be seen as a concept for total causality. In a VAR setting, Sims causality can be expressed in terms of the elements of the transfer matrix (see (2) and (3b)). According to these concepts, we provide now the following definitions of direct and total causality between scalar-valued and vector-valued processes.

Definition Given a vector stochastic process composed equivalently of Q scalar-valued processes and of M vector-valued processes, $Y(n) = \left[y_1(n) \cdots y_Q(n)\right] = \left[Y_1(n)^T \cdots Y_M(n)^T\right]^T$ with $Y_m = [y_{m_1} \cdots y_{m_{M_m}}]^T$, and admitting an AR representation as in (1), the following causality definitions are stated:

- *direct causality* from y_j to y_i, $y_j \rightarrow y_i$, occurs if $A_{ij}(k)$ is not uniformly zero for all $k > 0 (1 \leq i, j \leq Q, i \neq j)$;
- *total causality* from y_j to y_i, $y_j \Rightarrow y_i$, occurs if at least one cascade involving L direct causality relations and $L+1$ scalar processes exists such that $y_{q_0} \rightarrow \cdots \rightarrow y_{q_L}$ with $q_0 = j, q_L = i, \{q_1, \ldots, q_{L-1}\} \in \{1, \ldots, Q\} \backslash \{i, j\}$
- *direct causality* from Y_m to Y_l, $Y_m \rightarrow Y_l$, occurs if $y_j \rightarrow y_i$ for at least one $j \in \{m_1, \ldots, m_{M_m}\}$ and at least one $i \in \{l_1, ..., l_{M_l}\}$ $(1 \leq l, m \leq M, l \neq m)$
- *total causality* from Y_m to Y_l, $Y_m \Rightarrow Y_l$, occurs if $y_j \Rightarrow y_i$ for at least one $j \in \{m_1, ..., m_{M_m}\}$ and at least one $i \in \{l_1, ..., l_{M_l}\}$ $(1 \leq l, m \leq M, l \neq m)$;

In the time domain, testing for causality according to the above definitions can be done in a straightforward way, starting from the relations of direct causality between scalar-valued processes and checking whether groups of VAR coefficients are zero, e.g., using a Wald test (Lutkepohl 2005). In the frequency domain, tests for direct and total causality are performed by checking at different frequencies the statistical significance of properly defined causality measures. In the following sections we survey existing frequency domain measures of Granger causality and related concepts of total causal influence, and propose new measures valid for vector-valued multivariate processes. Nevertheless it is important to stress that, since the above definitions reflect the concepts of Granger and Sims causality for scalar- and vector-valued processes, they cannot be considered genuine descriptions of causality unless the investigated process is—in its AR representation—the actual data generating process. Note also that the validity of the total causality definitions is endangered by the possibility that multiple (direct and/or indirect) effects cancel out so that the total effect vanishes. In general, inference about the real causal structure about a multivariate process can be safely done only under the so-called completeness and faithfulness assumptions made in causal inference (see, e.g., Spirtes et al. 2000).

2.2 Frequency domain causality measures for multiple scalar-valued processes

When the considered processes are all scalar-valued (i.e., $Y_m(n) = y_m(n)$, $M_m = 1$ for each $m = 1, ..., M = Q$), the spectral density and its inverse become $M \times M$ matrices in which each element describes cross-spectral and inverse cross-spectral relations between two scalar-valued processes. Under the assumption of strict causality, the decomposition (4) becomes, for the i–j element of $\mathbf{S}(\omega)$ and $\mathbf{P}(\omega)$

$$S_{ij}(\omega) = \sum_{m=1}^{M} \sigma_{mm}^2 H_{im}(\omega) H_{jm}^*(\omega), \tag{5a}$$

$$P_{ij}(\omega) = \sum_{m=1}^{M} \frac{1}{\sigma_{mm}^2} \bar{A}_{mi}^*(\omega) \bar{A}_{mj}(\omega). \tag{5b}$$

where σ_{mm}^2 and $1/\sigma_{mm}^2$ are the m–m elements of the diagonal matrices $\boldsymbol{\Sigma}$ and $\boldsymbol{\Sigma}^{-1}$(σ_{mm}^2 is the variance of y_m). The decompositions in (5) lead to the definitions the DC (Baccala et al. 1998) and the PDC (Baccala et al. 2007; Baccala and Sameshima 2001) from y_j to y_i as the complex-valued frequency domain functions

$$\gamma_{ij}(\omega) = \frac{\sigma_{jj} H_{ij}(\omega)}{\sqrt{S_{ii}(\omega)}} \tag{6}$$

and

$$\pi_{ij}(\omega) = \frac{\frac{1}{\sigma_{ii}} \bar{A}_{ij}(\omega)}{\sqrt{P_{jj}(\omega)}}. \tag{7}$$

The squared modulus of the DC and PDC defined in (6) and (7), $|\gamma_{ij}(\omega)|^2$ and $|\pi_{ij}(\omega)|^2$, are computed to quantify the strength of the directed interaction occurring from y_j to y_i at the frequency ω, normalized between 0 and 1. Combining (5) and (6) one can see that the squared DC $|\gamma_{ij}(\omega)|^2$ measures causality as the relative amount of power of y_i which is received from y_j at the frequency f, while the squared PDC $|\pi_{ij}(\omega)|^2$ measures causality as the relative amount of inverse power of y_j which is sent to y_i at the frequency f. It can be shown (see Appendix) that the DC measures total causality (Eichler 2006), while the PDC measures direct causality (Baccala and Sameshima 2001; Gigi and Tangirala 2010), from one scalar-valued process to another in the multivariate representation. Moreover, the complex-valued DC and PDC constitute factors in the decomposition of the ordinary coherence, and of the partial coherence, respectively (Faes and Nollo 2011). Note that the quantity which we denote as PDC was named "generalized PDC" in Baccala et al. (2007), while the original version of the PDC (Baccala and Sameshima 2001) was not including inner normalization by the input noise variances; the definition in (7) follows directly from the decomposition in (5b), and satisfies the desirable property of scale-invariance.

2.3 Frequency domain causality measures for two vector-valued processes

When only $M = 2$ vector-valued processes $Y_1(n)$ and $Y_2(n)$ of dimension M_1 and M_2 are considered, the analysis framework becomes that introduced by Geweke (1982) and further developed and studied later on Chen et al. (2006) and Wang et al. (2007). In this case, the input–output representation of the overall process may be partitioned in terms of the two considered processes as

$$\begin{bmatrix} Y_1(\omega) \\ Y_2(\omega) \end{bmatrix} = \begin{bmatrix} \mathbf{H}_{11}(\omega) & \mathbf{H}_{12}(\omega) \\ \mathbf{H}_{21}(\omega) & \mathbf{H}_{22}(\omega) \end{bmatrix} \begin{bmatrix} U_1(\omega) \\ U_2(\omega) \end{bmatrix}, \tag{8}$$

where $Y_i(\omega)$ and $U_i(\omega)$ are the FTs of $Y_i(n)$ and $U_i(n)$, and $\mathbf{H}_{ij}(\omega)$ describes the transfer from U_j to Y_i in the frequency domain ($i, j = 1, 2$). Under the assumption of strict causality, the spectral factorization proposed in Gevers and Anderson (1981) holds also for the vector-valued processes, so that (4a) can be particularized as

$$\mathbf{S}_{ii}(\omega) = \mathbf{H}_{ii}(\omega)\mathbf{\Sigma}_{ii}\mathbf{H}^*_{ii}(\omega) + \mathbf{H}_{ij}(\omega)\mathbf{\Sigma}_{jj}\mathbf{H}^*_{ij}(\omega),$$
$$i, j = 1, 2 (i \neq j), \tag{9}$$

where $\mathbf{S}_{ii}(\omega)$ is the spectral density matrix associated to Y_i, and $\mathbf{\Sigma}_{ii}$ is the covariance of $U_i (\mathbf{\Sigma}_{ii} = E\left[U_i(n)U_i(n)^T\right])$. The first and second term on the right hand side of (9) can be interpreted as intrinsic power of Y_i and as causal power of Y_i due to Y_j, respectively. This interpretation leads to defining the linear feedback from Y_j to Y_i at the frequency ω as (Geweke 1982; Wang et al. 2007)

$$f_{j\to i}(\omega) = \ln \frac{|\mathbf{S}_{ii}(\omega)|}{\left|\mathbf{H}_{ii}(\omega)\mathbf{\Sigma}_{ii}\mathbf{H}^*_{ii}(\omega)\right|}, \quad i, j = 1, 2\ (i \neq j). \tag{10}$$

With this definition, the lower bound of the linear feedback measure f is 0, and is achieved when the whole power at a given frequency is intrinsic (i.e., the causal power is zero). Note that the index has no upper bound, as f diverges when the intrinsic power is zero (i.e., the whole power of Y_i is due to Y_j). It can be shown (see Appendix) that f measures either direct or total causality, which in this bivariate formulation are equivalent concepts, from one vector-valued process to the other. We note that, in the particular case of two scalar-valued processes ($M_1 = M_2 = 1$), the logarithmic measure (10) is related to the DC from y_j to y_i. In this case we have indeed:

$$f_{j\to i}(\omega) = \ln \frac{S_{ii}(\omega)}{\sigma^2_{ii}\left|H_{ii}(\omega)\right|^2} = \ln \frac{S_{ii}(\omega)}{S_{ii}(\omega) - \sigma^2_{ij}\left|H_{ij}(\omega)\right|^2}$$
$$= \ln \frac{1}{1 - \left|\gamma_{ij}(\omega)\right|^2}. \tag{11}$$

3 Frequency domain causality measures for multiple vector-valued processes

The frequency domain measures of causality surveyed in Sect. 2 account for Granger causal effects either between multiple scalar-valued processes ($M > 2$ but $M_m = 1$ for each $m = 1, \ldots, M$; Sect. 2.2), or between pairs of vector-valued processes ($M_m > 1$ but $M = 2$; Sect. 2.3). In this section we generalize the existing measures to allow quantification of causality between multiple vector-valued processes ($M > 2$, $M_m > 1$). The generalization will lead to measures of direct and total causality among multiple blocks of time series. To do this, we first generalize the Geweke's logarithmic measure of linear feedback (10) to multiple processes, showing that it reflects total causality and defining a dual logarithmic measure that reflects direct causality only. Then, we exploit the relations between logarithmic and non-logarithmic measures established for multiple scalar-valued processes to provide generalized definitions of non-logarithmic measures valid for multiple vector-valued processes.

3.1 Logarithmic measures

In the general case of multiple vector-valued processes all spectral, coefficient, and covariance matrices of dimension $Q \times Q$ (i.e., $\mathbf{S}(\omega)$, $\mathbf{P}(\omega)$, $\mathbf{A}(\omega)$, $\mathbf{H}(\omega)$, $\mathbf{\Sigma}$, $\mathbf{\Sigma}^{-1}$) can be expressed as composed of M^2 blocks, with the i–j block having dimension $M_i \times M_j$. Exploiting this property, the spectral factorizations in (4) can be further decomposed, under the assumption of strict causality, as

$$\mathbf{S}_{ii}(\omega) = \sum_{m=1}^{M} \mathbf{H}_{im}(\omega)\mathbf{\Sigma}_{mm}\mathbf{H}^*_{im}(\omega), \tag{12a}$$

$$\mathbf{P}_{jj}(\omega) = \sum_{m=1}^{M} \bar{\mathbf{A}}^*_{mj}(\omega)\mathbf{\Sigma}^{-1}_{mm}\bar{\mathbf{A}}_{mj}(\omega), \tag{12b}$$

where $\mathbf{S}_{ii}(\omega)$ and $\mathbf{P}_{jj}(\omega)$ are the spectral and inverse spectral matrices of $Y_i(n)$ and $Y_j(n)$, $\mathbf{H}_{im}(\omega)$ and $\bar{\mathbf{A}}_{mj}(\omega)$ are the i–m block and the m–j block of the frequency-domain transfer and coefficient matrices, and $\boldsymbol{\Sigma}_{mm}$ and $\boldsymbol{\Sigma}_{mm}^{-1}$ are the m–m block of the innovation process covariance matrix and of its inverse. Based on the decompositions in (12), we provide now definitions for logarithmic frequency domain measures of causality which hold for multiple blocks of processes.

Definition Given two vector stationary stochastic processes Y_i and Y_j taken from a multivariate set admitting AR and MA representation as in (1) and (2), the multivariate total linear feedback from Y_j to Y_i, $f_{j\to i}^{(\mathrm{m})}$, and the multivariate direct linear feedback from Y_j to Y_i, $g_{j\to i}^{(\mathrm{m})}$, are defined at the frequency ω as:

$$f_{j\to i}^{(\mathrm{m})}(\omega) = \ln \frac{|\mathbf{S}_{ii}(\omega)|}{\left|\mathbf{S}_{ii}(\omega) - \mathbf{H}_{ij}(\omega)\boldsymbol{\Sigma}_{jj}\mathbf{H}_{ij}^{*}(\omega)\right|}, \quad (13a)$$

$$g_{j\to i}^{(\mathrm{m})}(\omega) = \ln \frac{\left|\mathbf{P}_{jj}(\omega)\right|}{\left|\mathbf{P}_{jj}(\omega) - \bar{\mathbf{A}}_{ij}^{*}(\omega)\boldsymbol{\Sigma}_{ii}^{-1}\bar{\mathbf{A}}_{ij}(\omega)\right|}. \quad (13b)$$

The properties of these two logarithmic measures of causality are stated as follows (proofs are in the Appendix):

1. $f_{j\to i}^{(\mathrm{m})}(\omega) \geq 0$; in particular, $f_{j\to i}^{(\mathrm{m})}(\omega) = 0$ if $\mathbf{H}_{ij}(\omega) = 0$.
2. $g_{j\to i}^{(\mathrm{m})}(\omega) \geq 0$; in particular, $g_{j\to i}^{(\mathrm{m})}(\omega) = 0$ if $\bar{\mathbf{A}}_{ij}(\omega) = 0$.
3. $f_{j\to i}^{(\mathrm{m})}(\omega)$ reduces to the bivariate measure $f_{j\to i}(\omega)$ of (10) when only two vector-valued processes are present.
4. $f_{j\to i}^{(\mathrm{m})}(\omega)$ measures total causality from Y_j to Y_i at the frequency ω.
5. $g_{j\to i}^{(\mathrm{m})}(\omega)$ measures direct causality from Y_j to Y_i at the frequency ω.

In summary, the measure of total linear feedback (13a) extends to the case of multiple processes the Geweke's measure (10) which is defined only for two vector processes. The extension is meant to include into the "intrinsic power" of the destination process Y_i all causal power contributions coming from processes other than the source process Y_j, in a way such that causality is detected only when Y_i receives power from Y_j. As to the direct linear feedback measure (13b), its definition is based on a dual reasoning compared to that underlying the definition (13a). In this case causality is measured in terms of inverse spectral power flowing out from the source process, instead of spectral power flowing into the destination process. Both measures are non-negative, and take zero value in the absence of information transfer from Y_j to Y_i at the frequency ω; nonzero values are attained when the transfer matrix $\mathbf{H}_{ij}(\omega)$ (quantifying direct and/or direct effects), or the coefficient matrix $\bar{\mathbf{A}}_{ij}(\omega)$ (quantifying direct effects only) have at least one nonzero entry, documenting the existence of information transfer between at least one pair of the scalar processes that form Y_j and Y_i. We note that $f_{j\to i}^{(\mathrm{m})}(\omega)$ diverges at the frequency ω when the whole information transferred to Y_i at that frequency comes from Y_j (i.e., when $\mathbf{H}_{im}(\omega) = 0$ for each $m \neq j$), and that $g_{j\to i}^{(\mathrm{m})}(\omega)$ diverges when the whole information flowing out from Y_j goes directly to Y_i (i.e., when $\bar{\mathbf{A}}_{mj}(\omega) = 0$ for each $m \neq i$). Besides these cases, $f_{j\to i}^{(\mathrm{m})}$ and $g_{j\to i}^{(\mathrm{m})}$ are well defined for a given frequency ω when the matrices appearing in the denominator of (13a) and (13b) are non-singular at that frequency. This is the case for all frequencies when the overall process $Y(n)$ from which Y_i and Y_j are taken is of finite order, which is a common assumption in practice.

3.2 Non-logarithmic measures

The spectral decompositions in (12) can be seen as a generalization of the decompositions in (5), holding for scalar-valued processes, to multiple vector-valued processes. Pursuing this analogy, we provide now definitions for non-logarithmic frequency domain measures of direct and total causality which hold for multiple blocks of processes.

Definition Given two vector stationary stochastic processes Y_i and Y_j taken from a multivariate set admitting AR and MA representation as in (1) and (2), the block DC (bDC) and block PDC (bPDC) from Y_j to Y_i are the real-valued measures defined as follows

$$\gamma_{ij}^{(\mathrm{b})}(\omega) = 1 - \frac{\left|\mathbf{S}_{ii}(\omega) - \mathbf{H}_{ij}(\omega)\boldsymbol{\Sigma}_{jj}\mathbf{H}_{ij}^{*}(\omega)\right|}{|\mathbf{S}_{ii}(\omega)|}, \quad (14a)$$

$$\pi_{ij}^{(\mathrm{b})}(\omega) = 1 - \frac{\left|\mathbf{P}_{jj}(\omega) - \bar{\mathbf{A}}_{ij}^{*}(\omega)\boldsymbol{\Sigma}_{ii}^{-1}\bar{\mathbf{A}}_{ij}(\omega)\right|}{\left|\mathbf{P}_{jj}(\omega)\right|}. \quad (14b)$$

The definitions of bDC and bPDC were motivated by their relation with non-logarithmic frequency domain causality measures for vector multivariate processes. By comparing (13a) and (13b) with (14a) and (14b), one can indeed easily show that

$$f_{j\to i}^{(\mathrm{m})}(\omega) = \ln \frac{1}{1-\gamma_{ij}^{(\mathrm{b})}(\omega)} \quad , \quad g_{j\to i}^{(\mathrm{m})}(\omega) = \ln \frac{1}{1-\pi_{ij}^{(\mathrm{b})}(\omega)}. \quad (15)$$

Hence, the bDC $\gamma^{(\mathrm{b})}$ is related to the logarithmic measure of total causality $f^{(\mathrm{m})}$ in the same way as the bivariate DC is related to the Geweke's linear feedback measure particularized to scalar processes (see (11)), while a dual relation exists between the bPDC $\pi^{(\mathrm{b})}$ and the logarithmic measure of direct causality $g^{(\mathrm{m})}$.

The bDC and bPDC are well defined at each frequency ω whenever the overall process $Y(n)$ can be represented as a finite order stationary VAR process. As to their behavior, we show that bDC and bPDC possess properties similar to the traditional DC and PDC by stating the following properties (proofs are in the Appendix):

6. $0 \leq \gamma_{ij}^{(b)}(\omega) \leq 1$; in particular, $\gamma_{ij}^{(b)}(\omega) = 0$ if $\mathbf{H}_{ij}(\omega) = 0$ and $\gamma_{ij}^{(b)}(\omega) = 1$ if $\mathbf{H}_{im}(\omega) = 0$ for each $m \neq j$.
7. $0 \leq \pi_{ij}^{(b)}(\omega) \leq 1$; in particular, $\pi_{ij}^{(b)}(\omega) = 0$ if $\bar{\mathbf{A}}_{ij}(\omega) = 0$ and $\pi_{ij}^{(b)}(\omega) = 1$ if $\bar{\mathbf{A}}_{mj}(\omega) = 0$ for each $m \neq i$.
8. The bDC $\gamma_{ij}^{(b)}(\omega)$ reduces to the squared DC $|\gamma_{ij}(\omega)|^2$, and the bPDC $\pi_{ij}^{(b)}(\omega)$ reduces to the squared PDC $|\pi_{ij}(\omega)|^2$, when computed for two scalar processes.
9. The bDC $\gamma_{ij}^{(b)}(\omega)$ reduces to the cumulative squared DC, $\sum_{m=1}^{M_j} \left|\gamma_{ij_m}(\omega)\right|^2$, when the destination process Y_i is scalar.
10. The bPDC $\pi_{ij}^{(b)}(\omega)$ reduces to the cumulative squared PDC, $\sum_{m=1}^{M_i} \left|\pi_{i_m j}(\omega)\right|^2$, when the source process Y_j is scalar.
11. The bDC $\gamma_{ij}^{(b)}(\omega)$ measures total causality from Y_j to Y_i at the frequency ω.
12. The bPDC $\pi_{ij}^{(b)}(\omega)$ measures direct causality from Y_j to Y_i at the frequency ω.

Summarizing the above properties, the bDC and bPDC measures defined in (14) generalize to vector-valued processes the PDC and DC defined as in (6) and (7) for scalar-valued processes. They share many important properties of frequency domain measures of total causality and direct causality, while bringing the advantage coming to the fact that they summarize into a single coupling value the many directional interactions possibly existing among the scalar components of two vector process taken from a multivariate set.

4 Illustrative example

In this section, the frequency domain causality measures proposed for multiple vector-valued processes are illustrated by means of the exemplary eight-dimensional VAR process:

$$\begin{cases} y_1(n) = 2\rho\cos(2\pi f_1) y_1(n-1) - \rho^2 y_1(n-2) + u_1(n) \\ y_2(n) = k_1 y_1(n-1) + u_2(n) \\ y_3(n) = 2\rho\cos(2\pi f_3) y_3(n-1) - \rho^2 y_3(n-2) \\ \qquad +a_1 y_2(n-2) + d_1 y_8(n-2) + u_3(n) \\ y_4(n) = a_2 y_2(n-1) + u_4(n) \\ y_5(n) = c_1 y_3(n-1) + k_3 y_6(n-2) + u_5(n) \\ y_6(n) = c_2 y_3(n-2) + k_2 y_5(n-1) + u_6(n) \\ y_7(n) = c_3 y_3(n-1) + k_4 y_6(n-2) + u_7(n) \\ y_8(n) = b_1 y_3(n-2) + b_2 y_4(n-1) + u_8(n) \end{cases}, \quad (16)$$

where $U(n) = [u_1(n) \cdots u_8(n)]^T$ is a vector of uncorrelated white innovation processes of unitary variance (i.e., $\mathbf{\Sigma} = \mathbf{I}$). In the example, autonomous oscillations are obtained for the processes y_1 and y_3 representing them as second-order AR processes described by two complex-conjugate poles with modulus ρ and phase $\pm 2\pi f_{1,3}$ (in this study, $\rho = 0.9$, $f_1 = 0.1$, $f_3 = 0.25$). Moreover, direct causality is set between pairs of processes imposing the connections indicated in (16) and depicted in Fig. 1.

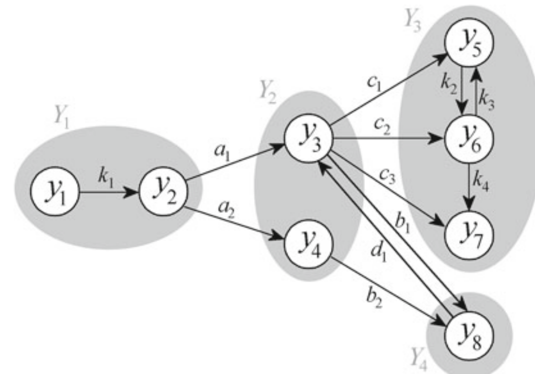

Fig. 1 Graphical representation of the VAR process described by (16). The $Q = 8$ scalar-valued processes $y_1, \ldots y_8$ compose the $M = 4$ vector-valued processes $Y_1, \ldots Y_4$ as depicted by the *gray* areas. Direct causal effects between two scalar-valued processes are shown by the *arrows*, with the corresponding parameter representing the weight of the connection

In this example, we assume that the $Q = 8$ scalar-valued processes $y_1, \ldots, y_8$ are the constituents of $M = 4$ vector-valued processes composed as: $Y_1 = [y_1 y_2]^T$, $Y_2 = [y_3 y_4]^T$, $Y_3 = [y_5 y_6 y_7]^T$, $Y_4 = y_8$. As shown in Fig. 1, interactions are set through the causal effects between pairs of scalar processes composing two different vector processes, i.e., from Y_1 to Y_2 (with parameters a_1, a_2), from Y_2 to Y_4 (with parameters b_1, b_2), from Y_2 to Y_3 (with parameters c_1, c_2, c_3), and from Y_4 to Y_2 (with parameter d_1). Moreover, the parameters k_1, k_2, k_3, k_4 determine "internal" effects for a single vector process, i.e., causal effects between pairs of scalar processes composing the same vector process. Except when stated otherwise, the values assumed in the analysis for the parameters are $a_1 = a_2 = 0.5$, $b_1 = b_2 = 0.4$, $c_1 = c_2 = c_3 = 0.4$, $d_1 = 0.7$, $k_1 = -0.5$, $k_2 = k_3 = k_4 = 0.5$.

4.1 Theoretical results

The theoretical profiles for the proposed logarithmic and non-logarithmic frequency domain causality measures, computed analytically according to (13) and (14), are reported in Fig. 2. First, we see that the profiles of the multivariate total feedback measure ($f_{j \to i}^{(m)}$, Fig. 2a) resemble those of the block DC ($\gamma_{ij}^{(b)}$, Fig. 2c), and that the profiles of the multivariate direct feedback measure ($g_{j \to i}^{(m)}$, Fig. 2b) resemble those of the block PDC ($\pi_{ij}^{(b)}$, Fig. 2d). These similarities in shape are due to

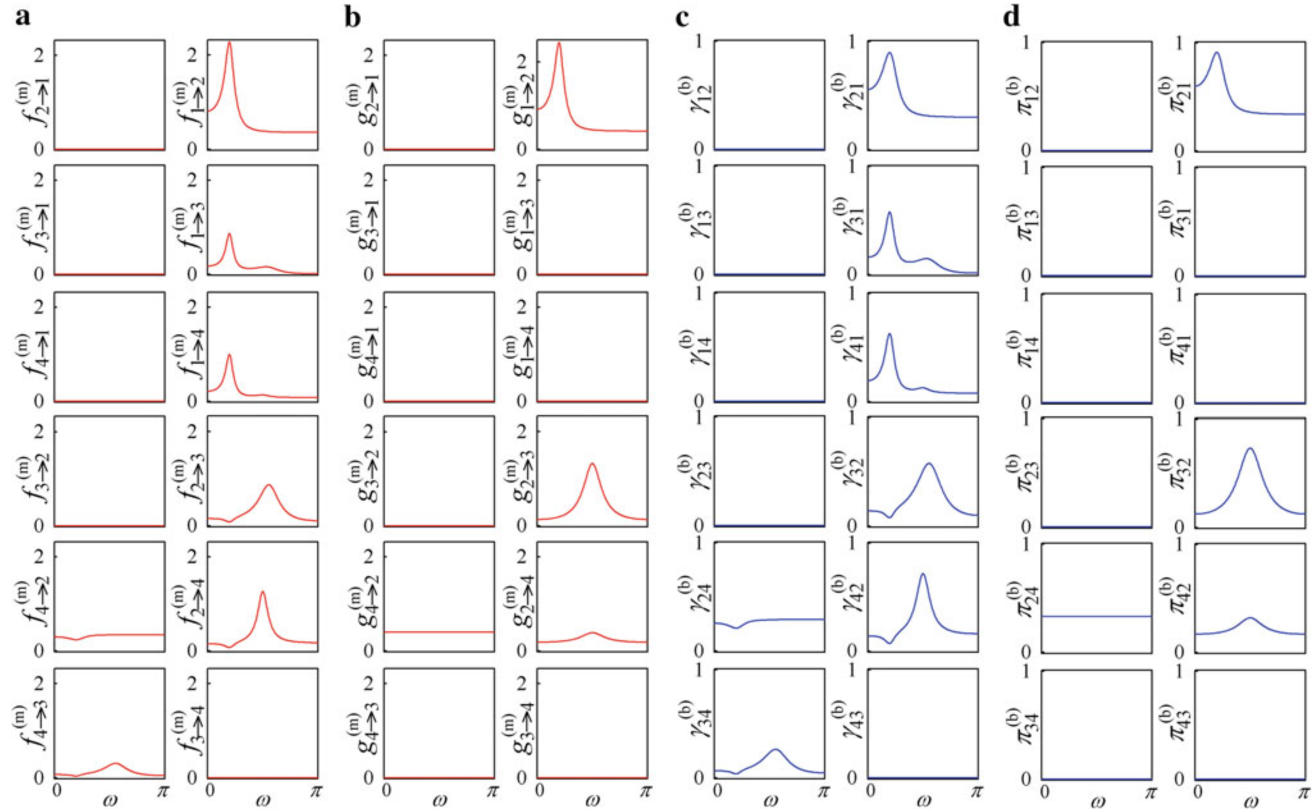

Fig. 2 Theoretical profiles of multivariate total causality $f_{j\to i}^{(m)}$ (**a**), multivariate direct causality $g_{j\to i}^{(m)}$ (**b**), bDC $\gamma_{ij}^{(b)}$ (**c**) and bPDC $\pi_{ij}^{(b)}$ (**d**) computed as a function of the frequency ω from the process Y_j to the process $Y_i (i, j = 1, \ldots, 4)$ for the illustrative example (16)

the dependencies between logarithmic and non-logarithmic causality measures stated in (15).

As seen in Fig. 2, all measures take non-negative values at all frequencies; in particular, the bDC and bPDC (Fig. 2c, d) are bounded between 0 and 1. In detail, the measures $g^{(m)}$ and $\pi^{(b)}$ elicit direct causality as they exhibit a nonzero profile only over the directions for which direct causality between two vector-valued processes is set (i.e., $Y_1 \to Y_2$, $Y_2 \to Y_3$, $Y_2 \to Y_4$, $Y_4 \to Y_2$, Fig. 2b, d), while being uniformly zero over all other directions. The measures $f^{(m)}$ and $\gamma^{(b)}$ reflect total causality, being nonzero at some frequencies whenever a cascade of direct causality relations is set from one vector-valued process to another (i.e., $Y_1 \to Y_2$, $Y_2 \to Y_3$, $Y_2 \to Y_4$, $Y_4 \to Y_2$; $Y_1 \to Y_2 \to Y_3$, $Y_1 \to Y_2 \to Y_4$, $Y_4 \to Y_2 \to Y_3$, Fig. 2a, c). This example shows the usefulness of the proposed measures for providing a compact representation of frequency domain causality in a network of vector processes. Note that similar structure determination would be less straightforward to attain using the traditional measures defined for scalar processes; for instance, the analysis of direct causality from Y_j to Y_i, if performed using the PDC, would require condensing in an arbitrary way the information provided by $M_i \times M_j$ squared PDC functions (see, e.g., middle and right columns of Fig. 3a).

As depicted in Fig. 2, causality relations among vector processes are reflected by the various measures with specific frequency-dependent behavior depending on the oscillations set for the driving process. Indeed, the oscillation set at $\omega_1 = 2\pi f_1 = \pi/5$ rad for the scalar process y_1, belonging to the vector process Y_1, is transmitted to Y_2, Y_3, and Y_4 according to the connections shown in Fig. 1, and is reflected by the peaks located at ω_1 for the causality measures $g_{1\to 2}^{(m)}$, $f_{1\to 2}^{(m)}$, $f_{1\to 3}^{(m)}$ $f_{1\to 4}^{(m)}$, and $\pi_{21}^{(b)}$, $\gamma_{21}^{(b)}$, $\gamma_{31}^{(b)}$, $\gamma_{41}^{(b)}$. In a similar way, the oscillation at $\omega_2 = 2\pi f_3 = \pi/2$ rad originated in Y_2 is transmitted to Y_3 and Y_4 and reflected by the peaks at ω_1 of the causality measures $g_{2\to 3}^{(m)}$, $g_{2\to 4}^{(m)}$, $f_{2\to 3}^{(m)}$, $f_{2\to 4}^{(m)}$ and $\pi_{32}^{(b)}$, $\pi_{42}^{(b)}$, $\gamma_{32}^{(b)}$, $\gamma_{42}^{(b)}$. This behavior, which describes the essence of a spectral density approach to causality analysis, may be lost if the study of a network of vector-valued processes is performed through the measures devised for the constituent scalar-valued variables. As an example, we report in Fig. 3 a comparison of PDC and bPDC analyses performed between Y_1 and Y_2 as in (16) with a relatively low coupling strength imposed from Y_1 to Y_2 (i.e., with $a_1 = a_2 = 0.2$). In this case, detection of direct causality $Y_1 \to Y_2$ appears a daunting task if performed on the basis of the corresponding direct causality relations involving the constituent scalar-valued processes (i.e., $y_2 \to y_3$ and

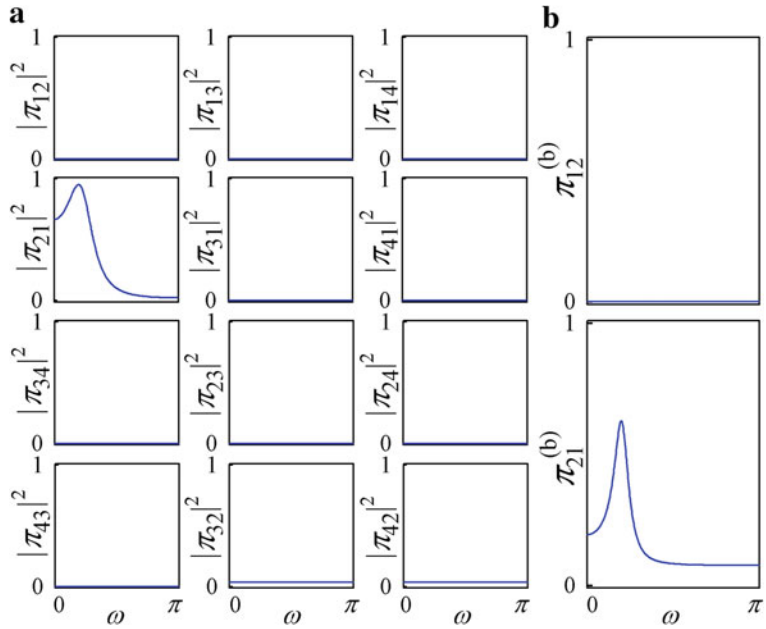

Fig. 3 Theoretical profiles of the twelve PDCs relevant to the vector processes $Y_1 = [y_1 \quad y_2]^T$ and $Y_2 = [y_3 \quad y_4]^T$ (**a** *first column* PDCs within Y_1 and Y_2; *middle and right columns* PDCs between Y_1 and Y_2) and corresponding bPDCs between Y_1 and Y_2 (**b**) computed for the illustrative example (16) with $a_1 = a_2 = 0.2$

$y_2 \rightarrow y_4$); indeed, the two PDCs $|\pi_{32}|^2$ and $|\pi_{42}|^2$ exhibit a flat profile with values very close to zero (Fig. 3a). On the contrary, the bPDC from Y_1 to Y_2, $\pi_{21}^{(b)}$, shows a clear nonzero profile with an evident peak at $\sim\pi/5$ rad (Fig. 3b). We ascribe the difference to the fact that the two PDCs do not consider the internal dynamics of the vector-valued source process Y_1, which in this case are very strong as documented by the sharp peak of $|\pi_{21}|^2$, while the bPDC takes these dynamics into account so that its profile from Y_1 to Y_2 is magnified by the important information transfer occurring within Y_1.

Figure 4 reports representative plots of the proposed measures computed at varying the coupling strength over some directions of interaction in the simulated network. As depicted in Fig. 4a, b, the measures take higher values at increasing the parameters that determine the causal coupling from one vector process to another. As an example, increasing the coupling from Y_2 to Y_3 through variation of the parameter c_1 from 0 to 1 determines a progressive increase of the bPDC from Y_2 to $Y_3(\pi_{32}^{(b)})$, as well as of the bDC from Y_1 to $Y_3(\gamma_{31}^{(b)}$, Fig. 4a). Similarly, the multivariate direct and total feedback measures $g_{1\rightarrow 2}^{(m)}$ and $f_{1\rightarrow 3}^{(m)}$ are uniformly zero in the absence of causal coupling from Y_1 to Y_2 ($a_1 = a_2 = 0$), and raise progressively when the causal coupling varies up to $a_1 = a_2$=1 (Fig. 4b). A different behavior is observed at varying the coupling strength between two scalar-valued processes belonging to the same vector-valued process. We note that direct and total causality measures are not affected by the variations of coupling parameters pertaining the destination vector process; this effect is documented by the overlapping profiles of the bPDC from Y_2 to Y_3 and the bDC from Y_1 to Y_3 obtained varying the coupling strength within Y_3 (i.e., acting on k_2 and k_3, Fig. 4c). On the contrary, causality measures are influenced by modifications of the causal coupling internal to the source process, as shown by the varying profiles of $g_{1\rightarrow 2}^{(m)}$ and $f_{1\rightarrow 3}^{(m)}$ resulting from coupling variations within Y_3 (i.e., from modifications of k_1, see Fig. 4d).

4.2 Practical implementation

In order to test the proposed frequency domain causality measures on simulated time series, we generated multiple realizations of the theoretical process (16), each lasting $N = 500$ points. Then, assuming no knowledge of the underlying system, a VAR model of order $p = 2$ was identified from each realization using a standard vector least squares approach (Faes et al. 2012). The estimated model coefficients and innovation covariance were used for computing numerically the logarithmic and non-logarithmic causality measures according to (13) and (14), in order to verify their agreement with the theoretical measures and to compare their frequency domain profiles with those of other available causality measures. Since the formulation of the proposed measures presupposes strict causality, their practical estimation was performed after forcing the input covariance $\mathbf{\Sigma}$ and its inverse $\mathbf{\Sigma}^{-1}$ to be diagonal matrices.

Figure 5 reports the results of the practical estimation of non-logarithmic measures of total causality (i.e., DC and bDC) computed over an exemplary direction of interaction between two vector process, i.e., from Y_1 to Y_3. The comparison between theoretical functions (red lines) and range of the estimated functions (mean ± SD over 100 realizations, blue lines) evidences that there is good agreement between

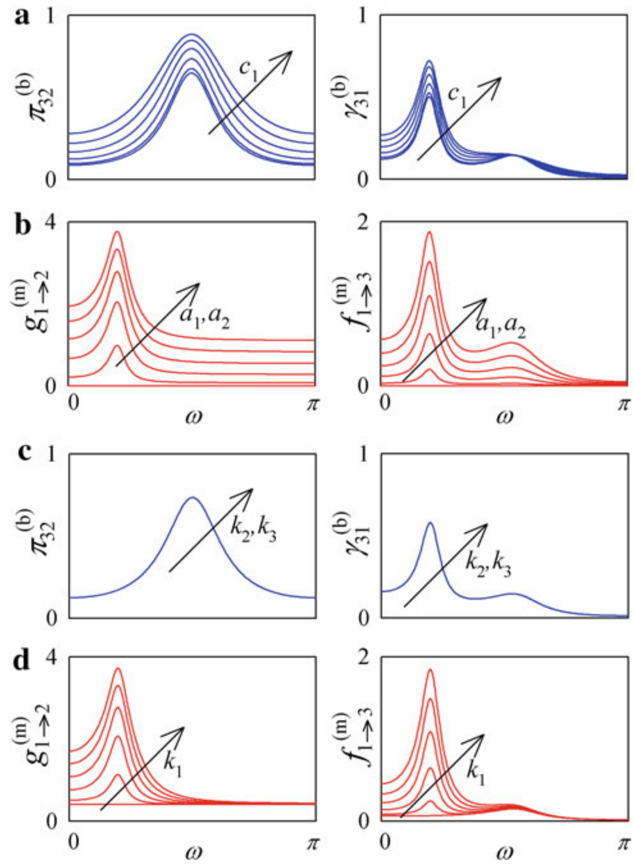

Fig. 4 Theoretical profiles of non-logarithmic (**a**,**c**, *blue*) and logarithmic (**b**,**d**, *red*) measures computed for the illustrative example (16) over selected representative directions, for different parameters values. For each *panel*, the parameters indicated in the plot were varied from 0 to 1, step 0.2, while all other parameters were kept constant ($a_1 = a_2 = 0.5$, $b_1 = b_2 = 0.4$, $c_1 = c_2 = c_3 = 0.4$, $d_1 = 0.7$, $k_1 = -0.5$, $k_2 = k_3 = k_4 = 0.5$). (Color figure online)

the two. The overall DC between the two vector processes is depicted by the ensemble of all the six functions linking $Y_1 = [y_1 y_2]^T$ to $Y_3 = [y_5 y_6 y_7]^T$ (Fig. 5a). To provide an overall indication of total causality from Y_1 to Y_3, one has to summarize in some way the information coming from the multiple DC functions; a reasonable choice is to compute the average DC, which is shown in Fig. 5b. As an alternative we may consider the bDC from Y_1 to Y_3 (Fig. 5c), which is computed without the need to elaborate several DC estimates; in this case, the bDC yields also a clear indication of the total causality relations existing at different frequencies, as documented by the more pronounced peaks exhibited in Fig. 5c compared with Fig. 5b.

Figure 6 reports the results of the statistical analysis testing the significance of direct causality, estimated using non-logarithmic measures (i.e., PDC and bPDC), over an exemplary direct connection between two vector-valued processes, i.e., $Y_2 \to Y_3$. The statistical analysis was performed comparing the PDC or bPDC functions with their

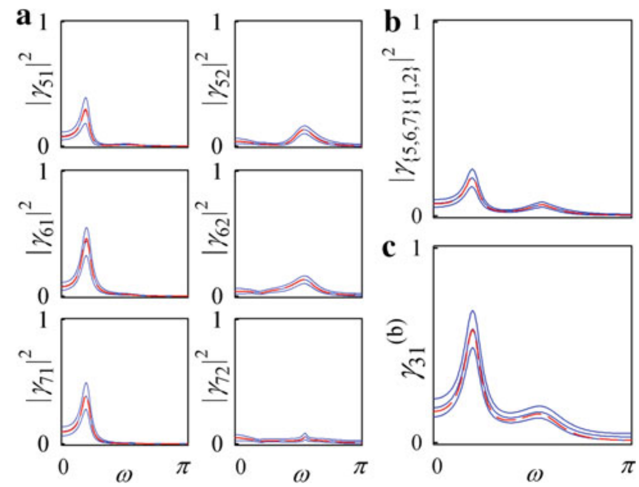

Fig. 5 Theoretical profiles (*red dashed*) and estimated profiles (*blue lines*, representing mean ± std. dev. of each function estimated over 100 process realizations) of the six DCs from $Y_1 = [y_1 \quad y_2]^T$ to $Y_3 = [y_5 \quad y_6 \quad y_7]^T$ (**a**) and of their average (**b**), as well as of the bDC from Y_1 to Y_3 (**c**). (Color figure online)

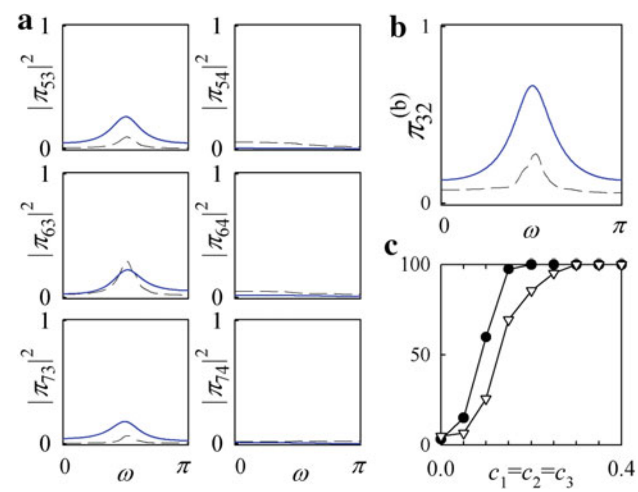

Fig. 6 Estimated profiles (*blue lines*) of the six squared PDCs from $Y_2 = [y_3 \quad y_4]^T$ to $Y_3 = [y_5 \quad y_6 \quad y_7]^T$ (**a**) and of the bPDC from Y_2 to Y_3 (**b**), computed for a single realization of the illustrative process along with their corresponding significance thresholds (*black dashed lines*). The rate of detection of significant direct causality from Y_2 to Y_3, expressed as the percentage of realizations for which at least one PDC was significant at $\omega = \pi/2$ (*white triangles*) or the percentage of realizations for which the bPDC was significant at $\omega = \pi/2$ (*black circles*), is reported in (**c**) as a function of the coupling strength (parameters $c_1 = c_2 = c_3$). (Color figure online)

corresponding frequency domain threshold for significance determined by means of a specific procedure based on the generation of surrogate data (Faes et al. 2010). The procedure, performed with significance α, estimates the frequency domain threshold for a given measure (PDC or bPDC) as the $100(1-\alpha)$th percentile of the distribution of the measure computed for multiple time series resembling the dynamical properties of the original series but lacking of causal

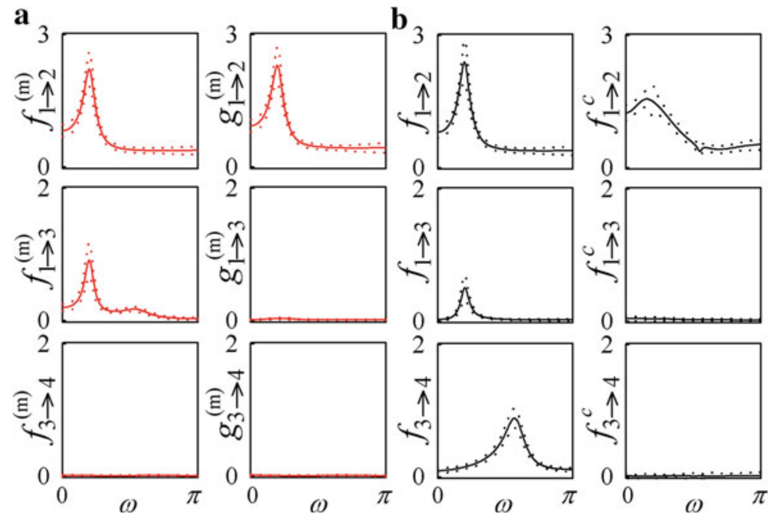

Fig. 7 Profiles of multivariate total causality $f^{(m)}$ and multivariate direct causality $g^{(m)}$ (**a**), and of Geweke's linear dependence f and conditional linear dependence f^c (**b**), estimated for three representative directions of interaction in the illustrative process (*top row* $Y_1 \rightarrow Y_2$; *middle row* $Y_1 \rightarrow Y_3$; *bottom row* $Y_3 \rightarrow Y_4$) and plotted as mean (*solid line*) ± std. dev. (*dotted lines*) over 100 realizations of the process

coupling over the direction of interaction; then, significant causality was detected when, at the frequency of interest, the measure exceeds the significance threshold. In the application depicted in Fig. 6 the procedure was performed with significance $\alpha = 0.05$, and a Bonferroni correction for multiple comparisons was applied for the PDC because in this case multiple PDC functions were computed between two vector processes. An example for a single realization of (16) is shown in Fig. 6a for the PDC (six functions) and in Fig. 6b for the bPDC (one block function). In this example, both approaches indicate the presence of significant direct causality at the frequency of the driving oscillation, since the PDCs $|\pi_{53}|^2$ and $|\pi_{73}|^2$, as well as the bPDC $\pi_{32}^{(b)}$, exceed the significance threshold at $\omega_2 = \pi/2$ rad. Figure 6c reports the results of the same statistical analysis repeated over 1000 realizations of the simulated process, and iterated at varying the strength of the direct coupling from Y_2 to Y_3 (strength variations are obtained setting $c_1 = c_2 = c_3$ at increasing values from 0 to 0.4). The analysis revealed a better performance of the bPDC, compared with repeated evaluations of the PDC, in detecting direct causality from Y_2 to Y_3, as it exhibits a higher detection rate in the presence of causality with weak coupling strength ($0 < c_1 = c_2 = c_3 < 0.3$).

Figure 7 reports an example of computation of the proposed logarithmic measures of causality, in comparison with existing previously proposed measures, for some exemplary directions of interaction between two vector process (i.e., from top to bottom, from Y_1 to Y_2, from Y_1 to Y_3, and from Y_3 to Y_4). As shown in Fig. 7a, the multivariate total linear feedback $f^{(m)}$ reflects both the direct effect $Y_1 \rightarrow Y_2$ and the indirect effect $Y_1 \rightarrow Y_2 \rightarrow Y_3$, while the multivariate direct linear feedback $g^{(m)}$ reflects the effect $Y_1 \rightarrow Y_2$ only. A comparison with the theoretical profiles in Fig. 2 indicates the good agreement with expected and estimated functions. To relate the proposed measures with existing block-based measures of causal interdependence, we report in Fig. 7b the corresponding estimated profiles of the Geweke's linear feedback measure (Geweke 1982; Wang et al. 2007, Eq. (10)) and conditional linear feedback measure (Chen et al. 2006; Geweke 1984) in the frequency domain. The bivariate measure f differs from our multivariate measure $f^{(m)}$ in the fact that it reflects not only direct and indirect causal effects, but also spurious effects due to non modeled variables: e.g., in our example, $f_{3\rightarrow4}$ has nonzero profile as a consequence of the simultaneous influence of Y_2—that is not considered in the computation of f—on both Y_3 and Y_4 (Fig. 7b), while $f^{(m)}_{3\rightarrow4}$ is uniformly zero at all frequencies. As to the conditional measure f^c, its profiles are similar to those of our multivariate measure of direct causality $g^{(m)}$, indicating that both measures are able to separate direct effects from indirect and spurious ones between two vector-valued processes.

5 Discussion and conclusion

The aim of the present study was to generalize to the analysis of multiple vector-valued processes existing frequency domain measures of directional connectivity that were proposed for multiple scalar-valued processes (Baccala and Sameshima 2001; Kaminski et al. 2001) or for pairs or triplets of vector-valued processes (Geweke 1982; Wang et al. 2007). The main advantage of the new measures over the existing ones lies in the fact that they provide a compact representation of the complex interaction structure of multivariate time series when they are organized in multiple blocks. With regard to the block DC and block PDC measures $\gamma^{(b)}$ and $\pi^{(b)}$, this peculiarity solves the issue of arbitrariness arising when several traditional DC or PDC functions linking the scalar constituents of two blocks of time series need to be summarized into a single causality measure. The way through which the block measures summarize the information about multiple causal relations is not only objective, but also non-trivial and efficient, as we have shown that bDC and bPDC are better able than DC and PDC to capture internal dependencies between the constituent series of a block (see, e.g., Fig. 3), exhibit more clear spectral profiles than simple averages of multiple scalar-valued functions (see, e.g., Fig. 5), and yield higher rates of causality detection for weakly coupled vector processes (see, e.g., Fig. 6). As regards the logarithmic measures, utilization of the full multivariate approach proposed in this study allows a straightforward representation of the whole structure of direct and total Granger causal relations with only one VAR model estimation, simplifying the interpretation and resulting less cumbersome than the repeated application of the bivariate or trivariate Geweke approaches (1982, 1984). Again, the full multivariate approach results are more efficient: the total causality measure $f^{(m)}$ is free from spurious effects that may arise using the Geweke bivariate measure f which is based on modeling two time series blocks only (see, e.g., Fig. 7); the direct causality measure $g^{(m)}$ can be computed from a single estimated VAR model, avoiding the complications related to the fitting of two different models which is required for computing the Geweke conditional causality measure f^{c} (Chen et al. (2006));

We have shown that the new measures are well defined under fairly general conditions, and possess other desirable properties of a frequency domain causality index. In particular, they are non-negative, are normalized between 0 and 1 in their non-logarithmic form, and are sensitive to variations of the coupling strength between two vector processes. An interesting observed feature is that the causality measures are not affected by coupling strength variations occurring within the destination vector process, whereas they increase at increasing the coupling strength within the source vector process (see Fig. 4). This is a desirable property, because coupling variations internal to the destination process should indicate how the incoming information flow is distributed within the constituent scalar processes, and thus one expects that they do not affect block causality measures. On the contrary, coupling variations internal to the source process are expected to be accounted for in a properly defined block causality measure as they correspond to variations in the information amount to be transmitted. This property extends to the context of time series and blocks a similar property of the measures valid for scalar time series: for instance, as the PDC is sensitive to the internal dynamics of the source scalar time series (i.e., dynamics occurring within the scalar series), the bPDC is sensitive to the internal dynamics of the source vector time series (i.e., dynamics occurring within and/or between the scalar constituents of the vector series). Note that, as a result of this property, the quantification of an indirect effect among scalar time series (e.g., performed through the DC) may resemble the quantification of a direct effect between vector time series (e.g., performed through the bPDC). However, this behavior does not contradict the interpretation of the bPDC as measures of direct causality, because—according to the definitions provided in Sect. 2.1—the existence of direct causality between blocks is determined only by the existence of direct Granger causal effects between the scalar constituents of two different blocks, and not by the effects between the scalar constituents of the same block.

From a theoretical point of view, the generalization to multiple vector-valued processes of logarithmic and non-logarithmic frequency domain causality measures aids the evaluation of their close reciprocal dependency. In fact, our extension of Geweke feedback measures and DC/PDC measures to multiple vector processes, together with the determination of their correspondence formalized in (15), extend relations that have been established only for pairs of scalar processes (Takahashi et al. 2010). Moreover, this result particularizes to the analysis of causality a very recent finding reported for the evaluation of coupling (i.e., non-causal connectivity) in the frequency domain, whereby logarithmic and non-logarithmic coupling measures were related to each other through the definition of the so-called "block-coherence" (Nedungadi et al. 2011). Our result states that the proposed causality measures provide essentially the same information in their logarithmic or non-logarithmic form. Specifically, $f^{(m)}$ and $\gamma^{(b)}$ on one side, and $g^{(m)}$ and $\pi^{(b)}$ on the other side, are strictly related with each other (see (15)) and thus exhibit similar frequency domain profiles (see, e.g., the example of Figs. 1, 2). Besides, we have demonstrated that the two pairs of measures capture different aspects of the causal information flow between two vector-valued processes belonging to a multivariate network: $f^{(m)}$ and $\gamma^{(b)}$ reflect both direct and indirect causal effects, thus helping to determine the total influence exerted by a process over another; $g^{(m)}$ and $\pi^{(b)}$ reflect direct effects only, thus helping to elucidate the interaction structure in complex networks composed of many processes.

The proposed measures are multivariate instances of Granger causality (Granger 1969, 1980) and related concepts of total causal influence (Sims 1972) computed from a strictly causal VAR model fitted on the observed set of time series. Although this framework for causality assessment is the most prominent and widely employed, especially in neuroscience, one should remark that it is exposed to the limitations peculiar of the specific concept of causality and model structure which underlie the derivation of the proposed measures. Granger causality is a probabilistic notion that differs from other operational definitions that have been used in the context of time series, such as intervention causality (Eichler 2012) and structural causality (White and Lu 2010). In general, interpreting Granger causality measures as causal effects is not possible and additional assumptions, such as requiring that the VAR model structure satisfies the causal Markov and faithfulness conditions, are necessary to infer true causal effects from probabilistic dependencies (Spirtes et al. 2000). In fact, a main limitation of causality analyses based on the Granger definition is that they can lead to the inference of spurious patterns of causality when important variables are not modeled. Hence, as with all Granger causality approaches, the detection of spurious causality becomes a major problem when the frequency domain measures proposed in this study are computed from systems that may be affected by latent variables. Another aspect to be considered is that the VAR modeling approach into which the proposed empirical analysis of Granger causality is framed covers only linear and time-invariant relationships between the observed time series. Recent advances in multivariate time series analysis have shown that modified model structures allow to deal with the confounding effects due to instantaneous correlations (Faes and Nollo 2010; Hyvarinen et al. 2010), latent variables (Eichler 2010; Guo et al. 2008), nonlinear effects (Marinazzo et al. 2011), and nonstationary behaviors (Sommerlade et al. 2012). Therefore, future developments should be aimed at extending the framework into which the proposed measures are defined, in order to deal with inherent properties of neurophysiological systems like the presence of instantaneous causality, time-varying relations, and nonlinear dynamics in the measured multiple blocks of time series.

In conclusion, the present study has established that the proposed frequency domain causality measures constitute a valid generalization of existing logarithmic and nonlogarithmic measures to multiple vector-valued processes. The presented generalized approach finds its natural application in the frequency-dependent characterization of directional interactions between multiple blocks of time series. This frame of applicability is very common in neurophysiology, where multichannel data acquisition technologies allow the simultaneous monitoring of several brain activity signals collected from many cortical regions of interest.

Appendix

In this Appendix we prove the properties stated for the new proposed frequency domain measures of causality for multiple vector processes. First, we demonstrate the properties of the non-logarithmic measures (i.e., bDC and bPDC, see (14)); then, we exploit the relation existing between logarithmic and non-logarithmic measures to demonstrate the properties of the measures defined in (13).

Properties 6 and 7 To determine the bounds of the bDC and bPDC functions, we first reformulate their definitions as follows. From (12a), the spectral density matrix of the vector process Y_i can be formulated as a sum of M contributions, $\mathbf{S}_{ii}(\omega) = \sum_{m=1}^{M} \mathbf{S}_{i|m}(\omega)$, with each contribution given by $\mathbf{S}_{i|m}(\omega) = \mathbf{H}_{im}(\omega)\Sigma_{mm}\mathbf{H}^*_{im}(\omega)$. This decomposition can be expressed separating the contribution to $\mathbf{S}_{ii}(\omega)$ coming from Y_j from all other contributions: $\mathbf{S}_{ii}(\omega) = \mathbf{S}_{i|j}(\omega)+\mathbf{S}_{i|-j}(\omega)$, with $\mathbf{S}_{i|-j}(\omega) = \sum_{m\neq j} \mathbf{S}_{i|m}(\omega)$. In a similar way, from (12b) the inverse spectral matrix of the vector process Y_j can be decomposed as $\mathbf{P}_{jj}(\omega) = \sum_{m=1}^{M} \mathbf{P}_{j\to m}(\omega)$, where $\mathbf{P}_{j\to m}(\omega) = \bar{\mathbf{A}}^*_{mj}(\omega)\mathbf{\Sigma}^{-1}_{mm}\bar{\mathbf{A}}_{mj}(\omega)$, and the sum can be further represented as $\mathbf{P}_{jj}(\omega) = \mathbf{P}_{j\to i}(\omega) + \mathbf{P}_{j\to -i}(\omega)$, with $\mathbf{P}_{j\to -i}(\omega) = \sum_{m\neq i} \mathbf{P}_{j\to m}(\omega)$. With this notation, the block DC and block PDC defined in (14a) and (14b) can be expressed as

$$\gamma_{ij}^{(\mathrm{b})}(\omega) = \frac{|\mathbf{S}_{ii}(\omega)| - |\mathbf{S}_{i|-j}(\omega)|}{|\mathbf{S}_{ii}(\omega)|},$$
$$\pi_{ij}^{(\mathrm{b})}(\omega) = \frac{|\mathbf{P}_{jj}(\omega)| - |\mathbf{P}_{j\to -i}(\omega)|}{|\mathbf{P}_{jj}(\omega)|}. \qquad (17)$$

Now we show that all matrices involved in (17) are positive semidefinite. To this end, we recall two known matrix properties (Berman and Shaked Monderer 2003): given two Hermitian positive semidefinite $n \times n$ square matrices $\mathbf{A}$ and $\mathbf{B}$, (a) the $m\times m$ matrix $\mathbf{C}=\mathbf{L}^*\mathbf{A}\mathbf{L}$ is positive semidefinite for any $n \times m$ matrix $\mathbf{L}$, and (b) the sum $\mathbf{D} = \mathbf{A} + \mathbf{B}$ is positive semidefinite. These properties can be proven recalling the definition of a semidefinite positive matrix, i.e., $\mathbf{A}$ is positive semidefinite if $X^*\mathbf{A}X \geq 0$ for any n-dimensional complex vector X, and showing that (a) for any m-dimensional complex vector Z we have that $Z^*\mathbf{C}Z = Z^*\mathbf{L}^*\mathbf{A}\mathbf{L}Z = X^*\mathbf{A}X \geq 0$ with $X = \mathbf{L}Z$; (b) for any n-dimensional complex vector X, $X^*\mathbf{D}X = X^*\mathbf{A}X + X^*\mathbf{B}X \geq 0$. In our case, $\mathbf{S}_{i|m}(\omega)$ and $\mathbf{P}_{j\to m}(\omega)$ are positive semidefinite according to property (a) since for strictly causal VAR processes the diagonal matrices $\mathbf{\Sigma}_{mm}$ and $\mathbf{\Sigma}^{-1}_{mm}$ have all positive diagonal elements, and thus are positive definite, for each $m = 1, \ldots, M$. It follows that, according to property (b), the matrix sums leading to $\mathbf{S}_{i|-j}(\omega)$ and $\mathbf{P}_{j\to -i}(\omega)$, as well as the total sums resulting in the matrices $\mathbf{S}_{ii}(\omega)$ and $\mathbf{P}_{jj}(\omega)$, are positive semidefinite.

Therefore, since the determinant of positive semidefinite matrices is always non-negative, we have $|\mathbf{S}_{ii}(\omega)| \geq 0$, $|\mathbf{P}_{jj}(\omega)| \geq 0$, $|\mathbf{S}_{i|-j}(\omega)| \geq 0$, $|\mathbf{P}_{j\to -i}(\omega)| \geq 0$. These conditions set the upper bound for the bDC and bPDC, i.e., $\gamma_{ij}^{(\mathrm{b})}(\omega) \leq 1$, $\pi_{ij}^{(\mathrm{b})}(\omega) \leq 1$. Moreover, exploiting the property $|\mathbf{A}+\mathbf{B}| \geq |\mathbf{A}| + |\mathbf{B}|$, valid for positive semidefinite matrices [derived from the Minkowski determinant theorem (Mirsky (1955)], we have also that $|\mathbf{S}_{ii}(\omega)| \geq |\mathbf{S}_{i|-j}(\omega)|$ and $|\mathbf{P}_{jj}(\omega)| \geq |\mathbf{P}_{j\to -i}(\omega)|$; these last conditions set the lower bound for bDC and bPDC, i.e., $\gamma_{ij}^{(\mathrm{b})}(\omega) \geq 0$, $\pi_{ij}^{(\mathrm{b})}(\omega) \geq 0$.

From the definitions in (14a) and (14b) it follows immediately that $\mathbf{H}_{ij}(\omega) = 0$ entails $\gamma_{ij}^{(\mathrm{b})}(\omega) = 0$ and $\bar{\mathbf{A}}_{ij}(\omega) = 0$ entails $\pi_{ij}^{(\mathrm{b})}(\omega) = 0$. Moreover, combining the definitions in (14) with the discussion above we see that the condition

$\mathbf{H}_{im}(\omega) = 0$ for each $m \neq j$ entails $\mathbf{S}_{i|-j}(\omega) = 0$, and thus $\gamma_{ij}^{(b)}(\omega) = 1$, and that the condition $\bar{\mathbf{A}}_{mj}(\omega) = 0$ for each $m \neq i$ entails $\mathbf{P}_{j\rightarrow -i}(\omega) = 0$, and thus $\pi_{ij}^{(b)}(\omega) = 1$. This completes the proof of properties 6 and 7.

Properties 8, 9, and 10 These properties describe how the bDC and bPDC can be expressed in terms of the corresponding traditional scalar causality measures, i.e., the DC and PDC, when one or both the interacting processes Y_i and Y_j are scalar. In particular, when the destination process Y_i is scalar, its dimension is $M_i = 1$, so that its spectral density is scalar (i.e., $\mathbf{S}_{ii}(\omega) = S_{ii}(\omega)$) and the product $\mathbf{H}_{ij}(\omega) \sum_{jj} \mathbf{H}_{ij}^*(\omega)$ becomes the scalar quantity $\sum_{m=1}^{M_j} \sigma_{j_m j_m}^2 \left|H_{ij_m}(\omega)\right|^2$, where $\sigma_{j_m j_m}^2$ and $H_{ij_m}(\omega)$ denote here the innovation variance of the m-th scalar process composing the input vector process Y_j, and the transfer function from such scalar process to the scalar output process Y_i. In this case, comparing (14a) with (6) we see that the bDC reduces to the cumulative squared DC:

$$\gamma_{ij}^{(b)}(\omega) = \frac{\sum_{m=1}^{M_j} \sigma_{j_m j_m}^2 \left|H_{ij_m}(\omega)\right|^2}{S_{ii}(\omega)} = \sum_{m=1}^{M_j} \left|\gamma_{ij_m}(\omega)\right|^2. \tag{18}$$

thus proving property 9. In a similar way, when the source process Y_j is scalar (i.e., $M_j = 1$), its inverse spectral density is also scalar ($\mathbf{P}_{jj}(\omega) = P_{jj}(\omega)$) and the product $\bar{\mathbf{A}}_{ij}^*(\omega) \sum_{ij}^{-1} \bar{\mathbf{A}}_{ij}(\omega)$ becomes the scalar quantity $\sum_{m=1}^{M_i} \left|\bar{A}_{i_m j}(\omega)\right|^2 \Big/ \sigma_{i_m i_m}^2$. Hence, in this case the bPDC reduces to the cumulative squared PDC from Y_j to the scalar processes that compose the output vector process Y_i:

$$\pi_{ij}^{(b)}(\omega) = \frac{\sum_{m=1}^{M_i} \left|\bar{A}_{i_m j}(\omega)\right|^2 \Big/ \sigma_{i_m i_m}^2}{P_{jj}(\omega)} = \sum_{m=1}^{M_i} \left|\pi_{i_m j}(\omega)\right|^2, \tag{19}$$

thus proving property 10. In the case in which both the source process Y_j and the destination process Y_i are scalar (i.e., $M_i = M_j = 1$), it follows immediately from (18) and (19) that the bDC and bPDC reduce to the squared modulus of the traditional DC and PDC, i.e., $\gamma_{ij}^{(b)}(\omega) = \left|\gamma_{ij}(\omega)\right|^2$ and $\pi_{ij}^{(b)}(\omega) = \left|\pi_{ij}(\omega)\right|^2$, thus proving property 8.

Properties 11 and 12 These properties state that the bPDC measures direct causality, while the bDC measures total causality, from one vector-valued process to another. First, we show that similar properties hold for the scalar-valued PDC and DC function. According to the definition of direct causality stated in Sect. 2.1, $y_j \rightarrow y_i$ when $A_{ij}(k)$ is nonzero for at least one value of $k (i \neq j)$; this entails, for some frequency ω, $\bar{A}_{ij}(\omega) = -A_{ij}(\omega) \neq 0$ and thus, according to (7), $\pi_{ij}(\omega) \neq 0$. As to the DC $\gamma_{ij}(\omega)$, it is possible to show that its numerator term $H_{ij}(\omega)$ can be expanded as a geometric series resulting in a sum of terms each one related to one of the (direct or indirect) transfer pathways connecting y_j to y_i (Eichler 2006). Therefore, $\gamma_{ij}(\omega)$ is nonzero whenever at least one path connecting y_j to y_i is significant, i.e., when $y_j \Rightarrow y_i$. These properties, when combined with the direct and total causality definitions stated for vector-valued processes, extend readily to the bPDC and bDC functions. Indeed, $Y_j \rightarrow Y_i$ entails that the matrix $\mathbf{A}_{ij}(k)$, of dimension $M_i \times M_j$, is nonzero for at least one value of k, so that $\bar{\mathbf{A}}_{ij}(\omega) = -\bar{\mathbf{A}}_{ij}(\omega) \neq 0$ for some frequency ω (see (3)) and thus, recalling that $P_{j\rightarrow i}(\omega)$ is positive semidefinite, $\left|\mathbf{P}_{j\rightarrow i}(\omega)\right| = \left|\bar{\mathbf{A}}_{ij}^*(\omega) \mathbf{\Sigma}_{mm}^{-1} \bar{\mathbf{A}}_{ij}(\omega)\right| > 0$. This determines $\left|\mathbf{P}_{j\rightarrow -i}(\omega)\right| < \left|\mathbf{P}_{jj}(\omega)\right|$ and, according to (17), $\pi_{ij}^{(b)}(\omega) > 0$. On the contrary, in the absence of direct causality from Y_j to Y_i we have $\mathbf{A}_{ij}(k) = 0$ for each k, so that $\bar{\mathbf{A}}_{ij}(\omega) = 0$, $\mathbf{P}_{j\rightarrow i}(\omega) = 0$, $\mathbf{P}_{j\rightarrow -i}(\omega) = \mathbf{P}_{jj}(\omega)$, and hence $\pi_{ij}^{(b)}(\omega) = 0$, thus completing the proof of property 11. Following a dual reasoning, property 12 is proved considering that total causality $Y_j \Rightarrow Y_i$ occurs when similar total causality relations are present between the constituent scalar processes of Y_j and Y_i, so that the transfer matrix $\mathbf{H}_{ij}(\omega)$ has at least one nonzero entry for some frequency ω. Therefore, the presence of total causality entails $|\mathbf{S}_{i|j}(\omega)| = |\mathbf{H}_{ij}(\omega) \sum_{jj} \mathbf{H}_{ij}^*(\omega)| > 0$, in a way such that $|\mathbf{S}_{i|-j}(\omega)| < |\mathbf{S}_{ii}(\omega)|$ and, from (17), $\gamma_{ij}^{(b)}(\omega) > 0$. On the contrary, in the absence of total causality we have $\mathbf{H}_{ij}(\omega) = 0$ for all ω, $\mathbf{S}_{i|j}(\omega) = 0$, $\mathbf{S}_{i|-j}(\omega) = \mathbf{S}_{ii}(\omega)$ and hence $\gamma_{ij}^{(b)}(\omega) = 0$.

Properties 1–5 The properties of the proposed logarithmic frequency domain causality measures can be deduced from the corresponding properties of the non-logarithmic measures, recalling the relationships between the two types of measures derived in (15). The conditions $f_{j\rightarrow i}^{(m)}(\omega) \geq 0$ and $g_{j\rightarrow i}^{(m)}(\omega) \geq 0$ (properties 1 and 2) follow from (15) and from the fact that $0 \leq \gamma_{ij}^{(b)}(\omega) \leq 1$ and $0 \leq \pi_{ij}^{(b)}(\omega) \leq 1$; in particular, when $\mathbf{H}_{ij}(\omega) = 0$ we have that $\gamma_{ij}^{(b)}(\omega) = 0$ (property 6) and thus $f_{j\rightarrow i}^{(m)}(\omega) = \ln 1 = 0$. while, when $\bar{\mathbf{A}}_{ij}(\omega) = 0$ we have that $\pi_{ij}^{(b)}(\omega) = 0$ (property 7) and thus $g_{j\rightarrow i}^{(m)}(\omega) = \ln 1 = 0$. Properties 4 and 5 follow directly from properties 11 and 12 and from the fact that $f_{j\rightarrow i}^{(m)}$ is zero (respectively, nonzero) if and only if $\gamma_{ij}^{(b)}(\omega)$ is zero (nonzero), while $g_{j\rightarrow i}^{(m)}$ is zero (nonzero) if and only if when $\pi_{ij}^{(b)}(\omega)$ is zero (nonzero). Finally, property 3 derives from the observation that when only $M = 2$ vector processes are present (12a) reduces to (9), and thus (13a) reduces to (10) (i.e., $f_{j\rightarrow i}^{(m)} = f_{j\rightarrow i}$).

References

Astolfi L, Cincotti F, Mattia D, Marciani MG, Baccala LA, De Vico FF, Salinari S, Ursino M, Zavaglia M, Ding L, Edgar JC, Miller GA, He B, Babiloni F (2007) Comparison of different cortical connectivity estimators for high-resolution EEG recordings. Hum Brain Mapp 28(2):143–157

Baccala LA, Sameshima K (2001) Partial directed coherence: a new concept in neural structure determination. Biol Cybern 84(7):463–474

Baccala LA, Sameshima K, Ballester G, Valle AC, Timo-Iaria C (1998) Studying the interaction between brain structures via directed coherence and Granger causality. Appl Signal Process 5:40–48

Baccala L, Sameshima K, Takahashi DY (2007) Generalized partial directed coherence. In: Proceedings of the 15th international conference on DSP, Cardiff, pp 163–166

Berman A, Shaked Monderer N (2003) Completely positive matrices. World Scientific, Singapore

Boudjellaba H, Dufour JM, Roy R (1992) Testing Causality Between 2 Vectors in Multivariate Autoregressive Moving Average Models. J Am Stat Assoc 87(420):1082–1090

Brovelli A, Ding M, Ledberg A, Chen Y, Nakamura R, Bressler SL (2004) Beta oscillations in a large-scale sensorimotor cortical network: directional influences revealed by Granger causality. Proc Natl Acad Sci USA 101(26):9849–9854

Chen Y, Bressler SL, Ding M (2006) Frequency decomposition of conditional Granger causality and application to multivariate neural field potential data. J Neurosci Methods 150(2):228–237

Chicharro D, Ledberg A (2012) When two become one: the limits of causality analysis of brain dynamics. PLoS One 7:e32466

Dhamala M, Rangarajan G, Ding M (2008) Analyzing information flow in brain networks with nonparametric Granger causality. Neuroimage 41(2):354–362

Ding L, Worrell GA, Lagerlund TD, He B (2007) Ictal source analysis: localization and imaging of causal interactions in humans. Neuroimage 34(2):575–586

Eichler M (2005) A graphical approach for evaluating effective connectivity in neural systems. Phil Trans R Soc B 360(1457):953–967

Eichler M (2006) On the evaluation of information flow in multivariate systems by the directed transfer function. Biol Cybern 94(7):469–482

Eichler M (2007) Granger causality and path diagrams for multivariate time series. J Econom 137(2):334–353

Eichler M (2010) Graphical causal modelling of multivariate time series with latent variables. J Mach Learn Res W&CP 9:193–200

Eichler M (2012) Causal inference in time series analysis. In: Berzuini C, Dawid P, Bernardinelli L (eds) Causality: statistical perspectives and applications. Wiley, Chichester, pp 327–354

Erla S, Faes L, Tranquillini E, Orrico D, Nollo G (2009) Multivariate autoregressive model with instantaneous effects to improve brain connectivity estimation. Int J Bioelectromagn 11(2):74–79

Faes L, Nollo G (2010) Extended causal modelling to assess partial directed coherence in multiple time series with significant instantaneous interactions. Biol Cybern 103(5):387–400

Faes L, Nollo G (2011) Multivariate frequency domain analysis of causal interactions in physiological time series. In: Laskovski AN (ed) Biomedical engineering. Trends in electronics, communications and software. InTech, Rijeka, pp 403–428

Faes L, Porta A, Nollo G (2010) Testing frequency domain causality in multivariate time series. IEEE Trans Biomed Eng 57(9): 1897–1906

Faes L, Erla S, Nollo G (2012) Measuring connectivity in linear multivariate processes: definitions, interpretation and practical analysis. Comput Math Methods Med 2012:140513(18pp)

Franaszczuk PJ, Bergey GK, Kaminski MJ (1994) Analysis of mesial temporal seizure onset and propagation using the directed transfer function method. Electroencephalogr Clin Neurophysiol 91(7):413–427

Gevers MR, Anderson BDO (1981) Representations of jointly stationary stochastic feedback processes. Int J Control 33(5):777–809

Geweke J (1982) Measurement of linear dependence and feedback between multiple time series. J Am Stat Assoc 77: 304–313

Geweke J (1984) Measures of conditional linear dependence and feedback between time series. J Am Stat Assoc 79:907–915

Gigi S, Tangirala AK (2010) Quantitative analysis of directional strengths in jointly stationary linear multivariate processes. Biol Cybern 103(2):119–133

Granger CWJ (1969) Investigating causal relations by econometric models and cross-spectral methods. Econometrica 37: 424–438

Granger CWJ (1980) Testing for causality: a personal viewpoint. J Econom Dynam Control 2:329–352

Guo SX, Seth AK, Kendrick KM, Zhou C, Feng JF (2008) Partial Granger causality—eliminating exogenous inputs and latent variables. J Neurosci Methods 172(1):79–93

Hsiao C (1982) Autoregressive modeling and causal ordering of economic variables. J Econom Dynam Control 4(3):243–259

Hyvarinen A, Zhang K, Shimizu S, Hoyer PO (2010) Estimation of a structural vector autoregression model using non-Gaussianity. J Mach Learn Res 11:1709–1731

Kaminski MJ, Blinowska KJ (1991) A new method of the description of the information flow in the brain structures. Biol Cybern 65(3):203–210

Kaminski M, Ding M, Truccolo WA, Bressler SL (2001) Evaluating causal relations in neural systems: granger causality, directed transfer function and statistical assessment of significance. Biol Cybern 85(2):145–157

Lizier JT, Prokopenko M (2010) Differentiating information transfer and causal effect. Eur Phys J B 73:605–615

Lutkepohl H (2005) New introduction to multiple time series analysis. Springer, Heidelberg

Marinazzo D, Liao W, Chen H, Stramaglia S (2011) Nonlinear connectivity by Granger causality. Neuroimage 58:330–338

Mirsky L (1955) An introduction to linear algebra. Clarendon Press, Oxford

Nedungadi AG, Ding MZ, Rangarajan G (2011) Block coherence: a method for measuring the interdependence between two blocks of neurobiological time series. Biol Cybern 104(3):197–207

Pereda E, Quiroga RQ, Bhattacharya J (2005) Nonlinear multivariate analysis of neurophysiological signals. Prog Neurobiol 77(1–2):1–37

Sato JR, Takahashi DY, Arcuri SM, Sameshima K, Morettin PA, Baccala LA (2009) Frequency domain connectivity identification: an application of partial directed coherence in fMRI. Hum Brain Mapp 30(2):452–461

Schelter B, Winterhalder M, Eichler M, Peifer M, Hellwig B, Guschlbauer B, Lucking CH, Dahlhaus R, Timmer J (2006) Testing for directed influences among neural signals using partial directed coherence. J Neurosci Methods 152(1–2):210–219

Sims CA (1972) Money, income and causality. American Economic Review 62:540–552

Sommerlade L, Thiel M, Platt B, Plano A, Riedel G, Grebogi C, Timmer J, Schelter B (2012) Inference of Granger causal time-dependent influences in noisy multivariate time series. J Neurosci Methods 203(1):173–185

Spirtes P, Glymour C, Scheines R (2000) Causation, prediction and search. MIT Press, Cambridge

Sporns O (2007) Brain Connectivity. Scholarpedia 2(11):4695

Takahashi DY, Baccala LA, Sameshima K (2010) Information theoretic interpretation of frequency domain connectivity measures. Biol Cybern 103(7):463–469

Tjostheim D (1981) Granger-causality in multiple time-series. J Econom 17(2):157–176

Toda HY, Phillips PCB (1993) Vector autoregressions and causality. Econometrica 61(7):1367–1393

Wang X, Chen YH, Bressler SL, Ding M (2007) Granger causality between multiple interdependent neurobiological time series: blockwise versus pairwise methods. Int J Neural Syst 17(2):71–78

White H, Lu X (2010) Granger causality and dynamic structural systems. J Financial Econom 8(2):193–243

Winterhalder M, Schelter B, Hesse W, Schwab K, Leistritz L, Klan D, Bauer R, Timmer J, Witte H (2005) Comparison directed of linear signal processing techniques to infer interactions in multivariate neural systems. Signal Process 85(12):2137–2160

Zhou ZY, Chen YH, Ding MZ, Wright P, Lu ZH, Liu YJ (2009) Analyzing brain networks with PCA and conditional Granger causality. Hum Brain Mapp 30(8):2197–2206